

**Anomalous Josephson Hall effect in doped topological insulators with nematic superconductivity**R. S. Akzyanov <sup>1,2,3</sup> and A. L. Rakhmanov <sup>1,3</sup><sup>1</sup>*Dukhov Research Institute of Automatics, Moscow 127055, Russia*<sup>2</sup>*Moscow Institute of Physics and Technology, Dolgoprudny, Moscow Region 141700, Russia*<sup>3</sup>*Institute for Theoretical and Applied Electrodynamics, Russian Academy of Sciences, Moscow 125412, Russia*

(Received 8 July 2022; accepted 17 November 2022; published 6 December 2022)

We study the physics of the Josephson effect in the odd-parity nematic superconductors within the Ginzburg-Landau approach. The order parameter is a two-component vector that transforms as a coordinate vector in the  $(x, y)$  plane under rotation and its direction is usually referred to as the nematicity direction. A nontrivial interplay between the nematicity and crystallographic axes of the superconductors that form the junction makes the Josephson effect quite unusual. We derive current-phase relations for different configurations of the junction, crystallographic axes of the sample, and the nematicity direction in the superconductors. We obtain that the Meissner kernel in the considered samples has off-diagonal components and the transverse phase difference across the junction can induce a Josephson current that flows along the contact. We show that such an anomalous Josephson Hall effect can be observed without any magnetization. We calculate the magnetic field dependence of the maximum current through the junction. We find that the period of the Fraunhofer oscillations of the maximum Josephson current depends on the geometry of the junction, the direction of the magnetic field, and the nematicity directions. The obtained results can be generalized to other superconductors with nondiagonal Meissner kernels.

DOI: [10.1103/PhysRevB.106.214502](https://doi.org/10.1103/PhysRevB.106.214502)**I. INTRODUCTION**

The Josephson effect is a general feature of superconducting phenomena [1–3]. It manifests itself as a generation of the supercurrent between two superconducting pieces that are separated by a thin barrier. The value of this current is controlled by the external gating that induces phase difference between superconductors. This effect not only is of importance for many superconducting devices but also provides important information about the physical nature of the superconducting order. The discovery of topological superconductivity opens a new prospect in Josephson physics [4]. In particular, the study of the Josephson currents in superconductor-ferromagnetic (SF) heterostructures gives rise to the observation of a set of new physical phenomena and the development of a new family of superconducting devices [5]. An important property of the SF systems is the possibility to govern the Josephson current by fine-tuning of magnetization of the F layer.

Recently, significant interest in transverse Josephson currents that flow along the junction [6–14] has arisen. This phenomenon is called the Josephson Hall effect, the anomalous Josephson Hall effect, or the tunnel Josephson Hall effect by an analogy with the anomalous Hall effect in the normal state [15]. The Josephson Hall effect arises due to nontrivial interplay between the magnetization and spin-orbit interaction [7,9–14] or unconventional superconductivity [6,8]. Such a transverse Josephson current can be comparable with the usual longitudinal Josephson current [14].

Experiments with doped topological insulators such as  $\text{Cu}_x\text{Bi}_2\text{Se}_3$  [16–22],  $\text{Sr}_x\text{Bi}_2\text{Se}_3$  [23–29], and  $\text{Nb}_x\text{Bi}_2\text{Se}_3$  [30–33] reveal in them a superconductivity below critical

temperature  $T_c \sim 3$  K. The breaking of the rotational symmetry in these superconductors has been observed experimentally [20,21,25,27,32] as well as the spin triplet character of the Cooper's pairing [22]. Such properties are best described if we assume that the superconducting order parameter is a two-component vector with  $E_u$  representation, which is usually called the nematic superconducting state [34–37].

The nematic superconductivity generated a great interest due to its unusual properties such as the existence of Majorana Kramer's pairs [38,39], vestigial nematic order [40], surface Andreev bound states [41], unconventional collective modes [42], spontaneous strain [43], unusual magnetic response [44], and anisotropic quasiparticle interference [45,46]. A majority of these effects are related to the vector nature of the order parameter. The orientation of the order parameter vector is often referred to as the nematicity direction and it controls the anisotropy axis of the system.

Naturally, an interesting Josephson physics is expected in such superconductors, which depends significantly on the mutual orientations of the nematicity axis and the junction plane. In Ref. [47] the authors discuss an idea of manipulation of the Josephson junction between a nematic  $\text{ABi}_2\text{Se}_3$  superconductor and a usual  $s$ -wave superconductor by the applied stress. Unusual behavior of the Josephson current in the contacts with nematic superconductors was suggested to be used for revealing of the nematic superconductivity and the study of the nature of the superconducting order [48].

In this work, we perform a study of the Josephson physics in nematic topological superconductors of the type  $\text{ABi}_2\text{Se}_3$  based on the phenomenological Ginzburg-Landau (GL) approach [35]. In Sec. II, we derive the GL equations for

such superconductors. We get that the Meissner kernel that shows the response of the supercurrent to the vector potential has off-diagonal components. In Sec. III, we consider a superconductor-insulator-superconductor (SIS) Josephson junction and derive current-phase relations for different orientations of the junction plane and crystallographic axes. We show that the anomalous Josephson Hall effect (that is, the Josephson current along the junction) can be observed in the system for a certain orientation of the contact plane to the crystal axes. In Sec. IV, we analyze the electromagnetic properties of the junction and derive the dependence of the maximum Josephson current through the junction on the magnetic field. In Sec. V, we discuss the obtained results.

## II. GINZBURG-LANDAU EQUATIONS

We start with the GL free energy  $F$  for the vector superconducting order parameter  $\vec{\eta} = (\eta_1, \eta_2)$ ,

$$F = F_0 + F_D + F_H, \quad (1)$$

where  $F_0$  is a homogeneous contribution,  $F_D$  is the gradient term, and  $F_H$  is a contribution due to the electromagnetic field. Following the seminal paper by Fu [35], we write down  $F_0$  in the form

$$F_0 = a(|\eta_1|^2 + |\eta_2|^2) + B_1(|\eta_1|^2 + |\eta_2|^2)^2 + B_2|\eta_1^*\eta_2 - \eta_1\eta_2^*|^2, \quad (2)$$

where  $a \propto T/T_c - 1 < 0$ ,  $B_1$  and  $B_2$  are the GL coefficients, and  $T_c$  is the critical temperature. The gradient term for the doped topological insulator of the type  $\text{ABi}_2\text{Se}_3$  can be chosen as [35,49]

$$F_D = J_1(D_i\eta_\alpha)^*D_i\eta_\alpha + J_3(D_z\eta_\alpha)^*D_z\eta_\alpha + J_4[(D_x\eta_1)^*D_x\eta_1 - (D_y\eta_1)^*D_y\eta_1] + (D_y\eta_2)^*D_y\eta_2 - (D_x\eta_2)^*D_x\eta_2 + (D_x\eta_1)^*D_y\eta_2 + (D_x\eta_2)^*D_y\eta_1 + (D_y\eta_1)^*D_x\eta_2 + (D_y\eta_2)^*D_x\eta_1]. \quad (3)$$

Here  $J_n$  are corresponding GL coefficients,  $D_j = -i\hbar\nabla_j - 2eA_j/c$ , summation over repeated indices  $i = x$  and  $y$  and  $\alpha = 1$  and  $2$  is assumed, and  $\mathbf{A} = (A_x, A_y, A_z)$  is the vector

potential. The magnetic part of the free energy reads

$$F_H = \frac{(\text{curl}\mathbf{A})^2}{8\pi} - \frac{\text{curl}\mathbf{A} \cdot \mathbf{H}_0}{4\pi}, \quad (4)$$

where  $\mathbf{H}_0$  is the applied field.

### A. First GL equations

The first GL equations can be obtained from the variation  $\delta F/\delta\eta_i^* = 0$ . This was done in many papers (see, e.g., Ref. [36]). We present here the result for the sake of completeness:

$$\hat{W}\vec{\eta} = 0, \quad (5)$$

$$\hat{W} = a + 2B_1\eta^2 + 2B_2\text{Im}(\eta_1^*\eta_2)\sigma_y + J_1(D_x^2 + D_y^2) + J_3D_z^2 + J_4(D_x^2 - D_y^2)\sigma_z + J_4[D_x, D_y]\sigma_x. \quad (6)$$

Here  $\sigma_j$  ( $j = 0, x, y, z$ ) are the Pauli matrices that act in  $\vec{\eta} = (\eta_1, \eta_2)$  space,  $\eta^2 = |\eta_1|^2 + |\eta_2|^2$ , and  $[D_x, D_y] = D_xD_y - D_yD_x$ . Boundary conditions for the first GL equations at the superconductor-vacuum interface read as follows:

$$J_1n_iD_i\eta_1 + J_3n_zD_z\eta_1 + J_4[n_xD_x\eta_1 - n_yD_y\eta_1 + n_xD_y\eta_2 + n_yD_x\eta_2] = 0, \quad (7)$$

$$J_1n_iD_i\eta_2 + J_3n_zD_z\eta_2 + J_4[n_yD_y\eta_2 - n_xD_x\eta_2 + n_xD_y\eta_1 + n_yD_x\eta_1] = 0, \quad (8)$$

where  $n_i = n_{x,y}$  and  $n_z$  are corresponding components of the external normal to the sample surface.

### B. Second GL equations

To derive the second GL equations, we perform variation of the GL functional with respect to the components of the vector potential. Here we present the results in the form convenient for calculation of the Josephson current. We start with variation of  $F_H$  and introduce, as usual, the current components

$$\delta_{\mathbf{A}}F_H = \frac{1}{c}\delta\mathbf{A}\mathbf{j}_s, \quad \mathbf{j}_s = \frac{c}{4\pi}\text{curl}\text{curl}\mathbf{A}. \quad (9)$$

In so doing, we obtain the second GL equations from the condition  $\delta_{\mathbf{A}}F = 0$  in the forms

$$j_{sz} = -2e\hbar J_3 \left[ F_{11}^z + F_{22}^z + \frac{4\pi}{\Phi_0} A_z (|\eta_1|^2 + |\eta_2|^2) \right],$$

$$j_{sx} = -2e\hbar \left\{ (J_1 + J_4) \left( F_{11}^x + \frac{4\pi}{\Phi_0} A_x \eta_1^* \eta_1 \right) + (J_1 - J_4) \left( F_{22}^x + \frac{4\pi}{\Phi_0} A_x \eta_2^* \eta_2 \right) + J_4 \left[ F_{12}^y + F_{21}^y + \frac{4\pi}{\Phi_0} A_y (\eta_1 \eta_2^* + \eta_1^* \eta_2) \right] \right\},$$

$$j_{sy} = -2e\hbar \left\{ (J_1 - J_4) \left( F_{11}^y + \frac{4\pi}{\Phi_0} A_y \eta_1^* \eta_1 \right) + (J_1 + J_4) \left( F_{22}^y + \frac{4\pi}{\Phi_0} A_y \eta_2^* \eta_2 \right) + J_4 \left[ F_{12}^x + F_{21}^x + \frac{4\pi}{\Phi_0} A_x (\eta_1 \eta_2^* + \eta_1^* \eta_2) \right] \right\}. \quad (10)$$

Here  $F_{\alpha\beta}^j = i\eta_\alpha^* \nabla_j \eta_\beta - i\eta_\beta \nabla_j \eta_\alpha^*$  and  $\Phi_0 = \pi\hbar c/e$  is the magnetic flux quantum. We introduce phases of the vector order parameter as  $\eta_1 = |\eta_1|e^{i\varphi_1}$ ,  $\eta_2 = |\eta_2|e^{i\varphi_2}$ ,  $\varphi = (\varphi_1 + \varphi_2)/2$ , and  $\delta = (\varphi_1 - \varphi_2)/2$ . We also express the order parameter components through a nematicity angle  $\alpha$  as  $|\eta_1| = \eta \cos \alpha$  and  $|\eta_2| = \eta \sin \alpha$ ,  $\alpha \in [0, \pi/2]$ . In these notations we have

$$F_{11}^j = -2\eta^2 \cos^2 \alpha \nabla_j \varphi_1, \quad F_{22}^j = -2\eta^2 \sin^2 \alpha \nabla_j \varphi_2,$$

$$F_{12}^j + F_{21}^j = -2\eta^2 (\sin 2\alpha \cos 2\delta \nabla_j \varphi - \sin 2\delta \nabla_j \alpha).$$

As a result, Eqs. (10) read as follows:

$$j_{sz} = 4e\hbar J_3 \eta^2 \left( \nabla_z \varphi + \cos 2\alpha \nabla_z \delta - \frac{2\pi}{\Phi_0} A_z \right), \quad (11)$$

$$j_{sx} = 4e\hbar \eta^2 \left\{ (J_1 + J_4 \cos 2\alpha) \left( \nabla_x \varphi - \frac{2\pi}{\Phi_0} A_x \right) + (J_1 \cos 2\alpha + J_4) \nabla_x \delta + J_4 \left[ \sin 2\alpha \cos 2\delta \left( \nabla_y \varphi - \frac{2\pi}{\Phi_0} A_y \right) - \sin 2\delta \nabla_y \alpha \right] \right\}, \quad (12)$$

$$j_{sy} = 4e\hbar \eta^2 \left\{ (J_1 - J_4 \cos 2\alpha) \left( \nabla_y \varphi - \frac{2\pi}{\Phi_0} A_y \right) + (J_1 \cos 2\alpha - J_4) \nabla_y \delta + J_4 \left[ \sin 2\alpha \cos 2\delta \left( \nabla_x \varphi - \frac{2\pi}{\Phi_0} A_x \right) - \sin 2\delta \nabla_x \alpha \right] \right\}. \quad (13)$$

These rather cumbersome equations can be rewritten in a compact form:

$$j_{si} = 4e\hbar \eta^2 \left[ v_i \left( \nabla_i \varphi - \frac{2\pi}{\Phi_0} A_i \right) + \gamma_i \nabla_i \delta + J_4 \sin 2\alpha \cos 2\delta \left( \nabla_{\bar{i}} \varphi - \frac{2\pi}{\Phi_0} A_{\bar{i}} \right) - J_4 \sin 2\delta \nabla_{\bar{i}} \alpha \right]. \quad (14)$$

Here  $i = (x, y, z)$  and  $\bar{i} = (y, x, 0)$ , which means that the two last terms are absent in the formula for  $j_{sz}$ ,  $(v_x, v_y, v_z) = (J_1 + J_4 \cos 2\alpha, J_1 - J_4 \cos 2\alpha, J_3)$  and  $(\gamma_x, \gamma_y, \gamma_z) = (J_1 \cos 2\alpha + J_4, J_1 \cos 2\alpha - J_4, J_3 \cos 2\alpha)$ .

Making the gradient transformation  $\mathbf{A} \rightarrow \mathbf{A} + \Phi_0 \nabla f / 2\pi$ , we restore the same Eq. (14) after the substitution  $\varphi \rightarrow \varphi + f$ . This means that  $\varphi_i$  transforms as  $\varphi_i \rightarrow \varphi_i + f/2$ . Note also that the phase difference  $\delta$  in the considered topological superconductors is a function of its internal properties and applied strain or magnetic field [35,36,43]. For example, if applied strain and/or magnetic field are absent we have a pure nematic phase with  $\delta = 0$  when  $B_2 > 0$  and a pure chiral phase with  $\delta = \pm\pi/4$  when  $B_2 < 0$ . The applied strain and/or magnetic field can transform the pure phase to some intermediate state with  $-\pi/4 < \delta < \pi/4$  [43].

From the obtained formulas it follows, in particular, that the supercurrent along the  $z$  direction is generated by the  $z$  component of the vector potential and/or the phase gradient along the  $z$  axis. However, in contrast to “usual” superconductors, the supercurrents along the  $x$  and  $y$  directions are generated by both  $A_x$  and  $A_y$  components of the vector potential and  $x$  and  $y$  components of the phase gradient, as well.

If we neglect variations of  $\eta_1$  and  $\eta_2$  in the bulk of the superconductor, we obtain the London equation for the nematic superconductor. In such a limit, it is convenient to rewrite Eq. (14) in the matrix form

$$\mathbf{j}_s = -\frac{c}{4\pi} \hat{K} \mathbf{A}, \quad \hat{K} = \frac{32\pi e^2 \eta^2}{c^2} \begin{pmatrix} v_x & \bar{J}_4 & 0 \\ \bar{J}_4 & v_y & 0 \\ 0 & 0 & v_z \end{pmatrix}, \quad (15)$$

where  $\bar{J}_4 = J_4 \sin 2\alpha \cos 2\delta$ . As we see, the Meissner kernel  $K_{\alpha\beta}$  has off-diagonal components  $K_{xy}$ , which is unusual. The  $K_{xy}$  terms in the Meissner kernel are inherent for superconductors anisotropic in the  $xy$  plane. The anisotropy arises in the superconducting state due to the vector nature of the order parameter. Note that the existence of the off-diagonal components of the Meissner kernel has been missed in previous microscopic calculations [50,51].

Substituting Eq. (15) in the corresponding Maxwell equation, we obtain the London equation for the nematic

superconductor:

$$\mathbf{H} + \text{curl}(\hat{K}^{-1} \text{curl}) \mathbf{H} = 0. \quad (16)$$

Since  $\hat{K}^{-1}$  has off-diagonal components, we have a mixing between  $H_x$  and  $H_y$  components of the magnetic field.

### III. CURRENT-PHASE RELATIONS

In this section, we obtain relations between the Josephson current through a SIS junction and the phases of the order parameter components when the external electromagnetic field is absent. The junction consists of two superconductors with the order parameters in the  $E_u$  representation. Superconducting correlations are induced by the proximity effect inside the junction  $-d/2 < z < d/2$ . We assume that these correlations are weak [52] and we can keep only quadratic in  $\eta_i \eta_j$  terms, neglecting terms of the fourth order that lead to the linearized GL equations that we obtain from Eq. (1). Following a standard approach, we assume that the GL coefficient in the junction  $a_N = a > 0$  is positive. We introduce another variable to emphasize that this coefficient refers to proximity-induced superconductivity in the junction.

#### A. Junction transverse to the $z$ direction

Consider a junction transverse to the  $z$  direction, which we call further the  $z$  junction (see Fig. 1). Inside the junction  $-d/2 < z < d/2$  the linearized GL equation (5) reads as

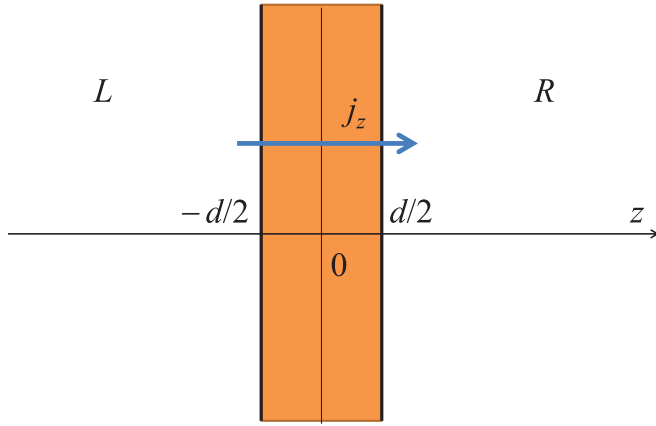
$$\nabla_z^2 \bar{\eta} = \frac{a_N}{\hbar^2 J_3} \bar{\eta}. \quad (17)$$

We use subscript  $L$  for the parameters at the left ( $z < 0$ ) of the junction and  $R$  for the parameters at the right ( $z > 0$ ). We set the boundary conditions  $\eta_j(+d/2) = \eta_{jR}$  and  $\eta_j(-d/2) = \eta_{jL}$  and obtain

$$\eta_j = \frac{(\eta_{jR} + \eta_{jL}) \cosh \kappa_z z}{2 \cosh(\kappa_z d/2)} + \frac{(\eta_{jR} - \eta_{jL}) \sinh \kappa_z z}{2 \sinh(\kappa_z d/2)}, \quad (18)$$

where  $\kappa_z = \sqrt{a_N/\hbar^2 J_3}$ . We substitute this formula into Eq. (14) for the supercurrent along the  $z$  axis and derive

$$j_z = j_{cz} [\cos \alpha_R \cos \alpha_L \sin \theta_1 + \sin \alpha_R \sin \alpha_L \sin \theta_2], \quad (19)$$

FIG. 1. Junction transverse to the  $z$  direction.

where  $\theta_j = \varphi_{jR} - \varphi_{jL}$  and

$$j_{cz} = \frac{4e\hbar J_3 \kappa_z \eta_R \eta_L}{\sinh \kappa_z d}. \quad (20)$$

We see that the Josephson current through the junction is a sum of contributions from two components of the order parameter. This relation differs from a general current-phase relation for usual two-band superconductors [53] since the phases of the order parameter components in the nematic superconductors are not independent [35]. It is reasonable to express the Josephson current in terms of the sum and difference of the phases of the order parameter components:

$$j_z = j_{cz} [\cos(\alpha_R - \alpha_L) \sin \theta \cos \phi + \cos(\alpha_R + \alpha_L) \cos \theta \sin \phi], \quad (21)$$

where  $\theta = \varphi_R - \varphi_L$  and  $\phi = \delta_R - \delta_L$ . We can tune the value of the Josephson current varying the nematicity direction. For example, in the case of the Josephson junction between two purely nematic superconductors  $\delta_L = \delta_R = 0$ , expression for the Josephson current takes a simple form,  $j_z = j_{cz} \cos(\alpha_R - \alpha_L) \sin \theta$ . We see that if the vector order parameters at different sides of the contact are orthogonal,  $\alpha_R - \alpha_L = \pi/2$ , there is no current through the junction,  $j_z = 0$ . In other terms,  $j_z = 0$  if  $\vec{\eta}_R = \eta_R(1, 0)$  and  $\vec{\eta}_L = \eta_L(0, 1)$  or vice versa  $\vec{\eta}_R = \eta_R(0, 1)$  and  $\vec{\eta}_L = \eta_L(1, 0)$ .

As usual for the Josephson effect, we assume that the density of the superconducting current in the bulk is much larger than the Josephson critical current density [1–3]. That is, the London penetration depth  $\lambda$  is much larger than the Josephson penetration depth  $\lambda_J$ . To estimate  $\lambda_J$  we need equations for the junction in the magnetic field obtained below in Sec. IV. Here we only note that the condition  $\lambda \ll \lambda_J$  requires  $\kappa_z d \gg 1$ ; that is, the contact is far from a superconducting transition, and the value  $\eta(z=0)$  is much smaller than the equilibrium order parameter in the bulk,  $\eta(|z| > d/2)$ .

### B. Junction transverse to the $x$ direction

Here we consider a junction transverse to the  $x$  axis, the  $x$  junction (see Fig. 2). The case of the  $y$  junction is a similar. The linearized first GL equation (5) in the junction

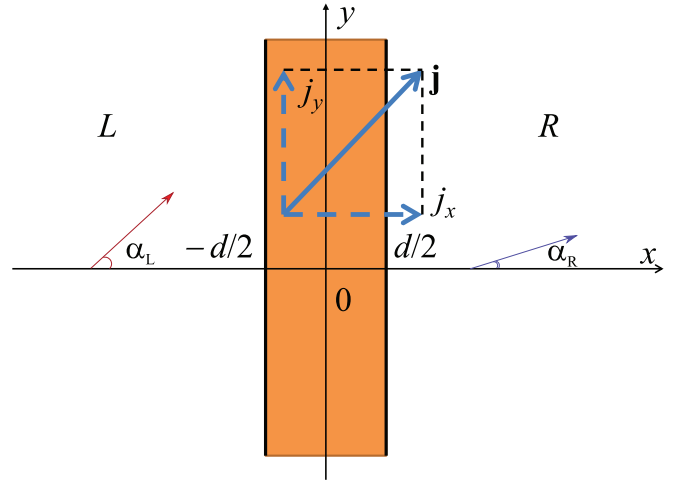


FIG. 2. Junction transverse to the  $x$  axis. Nematicity angles  $\alpha_L$  and  $\alpha_R$  show the direction of the vector of the order parameter,  $\delta_{L(R)} = 0$ .

$-d/2 < x < d/2$  is

$$\nabla_x^2 \vec{\eta} = \frac{(J_1 - J_4 \sigma_z) a_N}{\hbar^2 (J_1^2 - J_4^2)} \vec{\eta}. \quad (22)$$

We set boundary conditions  $\eta_j(+d/2) = \eta_{jR}$  and  $\eta_j(-d/2) = \eta_{jL}$  and derive

$$\eta_j = \frac{(\eta_{jR} + \eta_{jL}) \cosh \kappa_j x}{2 \cosh(\kappa_j d/2)} + \frac{(\eta_{jR} - \eta_{jL}) \sinh \kappa_j x}{2 \sinh(\kappa_j d/2)}, \quad (23)$$

where  $\kappa_1 = \sqrt{a_N/\hbar(J_1 + J_4)}$  and  $\kappa_2 = \sqrt{a_N/\hbar(J_1 - J_4)}$ . We substitute Eq. (23) in the formula for the components of the supercurrent, Eqs. (14). We observe that in the considered geometry the Josephson current through the junction has two components, usual current through the junction  $j_x$ , and transverse or Hall current along it,  $j_y$ . For the current through the contact we obtain

$$j_x = j_{c1} \cos \alpha_R \cos \alpha_L \sin \theta_1 + j_{c2} \sin \alpha_R \sin \alpha_L \sin \theta_2, \\ j_{c1} = \frac{4e\hbar(J_1 + J_4)\kappa_1\eta_L\eta_R}{\sinh \kappa_1 d}, \quad j_{c2} = \frac{4e\hbar(J_1 - J_4)\kappa_2\eta_L\eta_R}{\sinh \kappa_2 d}. \quad (24)$$

As in the case of the  $z$  junction,  $j_x$  consists of two terms, which correspond to two components of the order parameter, but in contrast to the previous case, the critical values of the current for  $\eta_1$  and  $\eta_2$  are different. Similar to Eq. (21), we can rewrite the latter formula in terms of  $\theta$  and  $\phi$ :

$$j_x = (j_{c1} \cos \alpha_R \cos \alpha_L + j_{c2} \sin \alpha_R \sin \alpha_L) \sin \theta \cos \phi + (j_{c1} \cos \alpha_R \cos \alpha_L - j_{c2} \sin \alpha_R \sin \alpha_L) \cos \theta \sin \phi. \quad (25)$$

As in the case of the  $z$  junction, we can tune the current value and even “turn off” the contact (that is, to put  $j_x = 0$ ) by a proper choice of the nematicity direction. As an example, consider a junction formed by two purely nematic superconductors,  $\delta_R = \delta_L = \phi = 0$ . In this case,  $j_x = 0$  if the

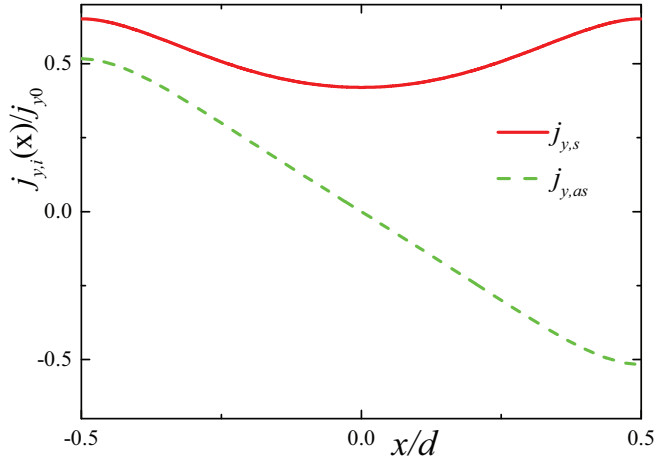


FIG. 3. Dependence of the symmetric  $j_{y,s}$  (red line) and anti-symmetric  $j_{y,as}$  (green dashed line) components of the transverse current  $j_y(x)/j_{y0}$  on the coordinate  $x$  for  $J_4/J_1 = 3/4$ ,  $k_1d = 5$ . Here  $j_{y0} = 4e\hbar J_4$ .

nematicity direction on right and left sides of the junction are perpendicular, just similar to the case of the  $z$  junction.

According to Eq. (14), in addition to  $j_x$ , we have a Josephson Hall current  $j_y$  flowing along the junction. The presence of such a transverse current is a direct consequence of the non-diagonal Meissner kernel and is an analog of the anomalous Josephson Hall effect [6–14]. Using Eqs. (10) and (23) we obtain

$$j_y = 4e\hbar J_4 \text{Im}(\eta_1^* \nabla_x \eta_2 + \eta_2^* \nabla_x \eta_1). \quad (26)$$

The current  $j_y$  depends on  $x$ . In the case of two nematic superconductors, the function  $j_y(x)$  can be presented as  $j_y(x) = j_{y,s}(x) \sin(\alpha_R + \alpha_L) + j_{y,as}(x) \sin(\alpha_R - \alpha_L)$ , where  $j_{y,s}(x) = j_{y,s}(-x)$  is a symmetric component of the current and  $j_{y,as}(x) = -j_{y,as}(-x)$  is antisymmetric. As we see, tuning of  $\alpha_R$  and  $\alpha_L$  can give us purely symmetric or antisymmetric current. In general, the transverse current  $j_y$  can be of the same order or even larger (for  $\delta > 0$ ) than  $j_x$ . Moreover,  $j_y$  can be nonzero when the current through the junction  $j_x$  is zero. The coordinate dependence of the symmetric and anti-symmetric parts of the current  $j_y(x)$  is illustrated in Fig. 3. The dependence of these components of the current on the junction thickness  $d$  is shown in Fig. 4. It is interesting to note that  $j_{y,as}(d)$  first grows with  $d$ , attains a maximum, and finally decreases, while  $j_{y,s}(d)$  decreases monotone from maximum at small  $d$  to zero, when  $\kappa_1 d \gg 1$ , as is common for Josephson currents [1]. Consider the case of the junction between two nematic superconductors,  $\delta_R = \delta_L = 0$ . To compare  $j_y$  and  $j_x$ , we introduce an average value:

$$\bar{j}_y = \frac{1}{d} \int_{-d/2}^{d/2} j_y(x) dx. \quad (27)$$

After straightforward calculations we derive

$$\bar{j}_y = j_{cy} \sin \theta, \quad (28)$$

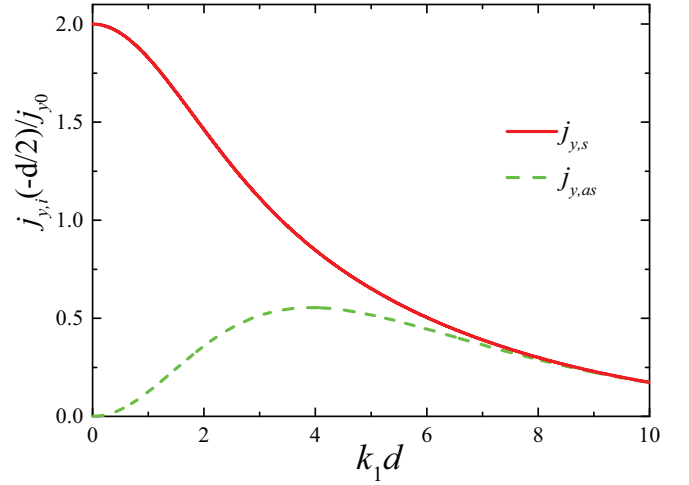


FIG. 4. Dependence of the symmetric  $j_{y,s}$  (red line) and anti-symmetric  $j_{y,as}$  (green dashed line) components of the transverse current  $j_y(x)/j_{y0}$  on  $k_1d$  for  $J_4/J_1 = 3/4$  at the left side of the contact  $x = -d/2$ . Here  $j_{y0} = 4e\hbar J_4$ .

where

$$j_{cy} = \sin(\alpha_R + \alpha_L) \frac{8e\hbar\eta^2 \sqrt{J_1^2 - J_4^2}}{d \sinh(\kappa_1 d) \sinh(\kappa_2 d)} \times (\cosh \kappa_2 d - \cosh \kappa_1 d). \quad (29)$$

In the case of two nematic superconductors  $\delta_R = \delta_L = 0$ ,  $j_y$  and  $j_x$  are typically of the same order for  $\kappa_1 d \sim 1$  and  $j_{cy}/j_{cx} \sim \tan \alpha / \kappa_1 d$  for  $\kappa_1 d \gg 1$ . The value of the Hall current  $\bar{j}_y$  is zero in the follows cases: (i) if  $J_4 = 0$  (that is,  $\kappa_1 = \kappa_2$ ) and the anisotropy is absent in the  $(x, y)$  plane, and (ii) if  $\alpha_R + \alpha_L = 0$  or  $\alpha_R + \alpha_L = \pi$ .

#### IV. JUNCTION IN THE MAGNETIC FIELD

In this section, we consider the junction in the magnetic field  $\mathbf{H}$ . As usual for Josephson physics, we assume that  $\mathbf{H}$  lies in the contact plane. We consider here only the case of two purely nematic superconductors,  $\delta_L = \delta_R = 0$ . Nonzero  $\delta$  results in the existence of an additional magnetization in the superconductor (see Ref. [43]), which, in general, should be included in the Maxwell equations. Also, finite  $\delta$  leads to the presence of the antisymmetric component in the current along the junction [see the text after Eq. (26)]. These effects deserve a separate detailed study in future work.

##### A. $z$ junction

First, we consider the junction, which lies in the plane  $(x, y)$  transverse to the  $z$  axis. Since the problem has rotational symmetry in the  $(x, y)$  plane we can choose the  $y$  axis along the direction of the applied magnetic field,  $\mathbf{H}_0 = (0, H_0, 0)$ . The magnetic field in the junction,  $z = 0$ , is  $\mathbf{H}(x, y) = [0, H(x, y), 0]$  and

$$\nabla_x H(x, y) = \frac{4\pi}{c} j_z, \quad (30)$$

where  $j_z$  is the current through the junction.

First, we consider the case without Josephson currents. The magnetic field in the bulk of the superconductor,  $\mathbf{H}(z) = [H_x(z), H_y(z), 0]$ , we can find using the London equation (16). In this limit we have

$$\begin{aligned}\nabla_z^2 H_x &= \frac{32\pi e^2 \eta^2}{c^2} (v_y H_x - \bar{J}_4 H_y), \\ \nabla_z^2 H_y &= \frac{32\pi e^2 \eta^2}{c^2} (v_x H_y - \bar{J}_4 H_x),\end{aligned}$$

and the dependence of  $\mathbf{H}$  on  $x$  is weak. The solution of these systems decays when  $z \rightarrow \pm\infty$  and  $\mathbf{H}(z=0) = [0, H(x, y), 0]$ . In the considered case  $\delta = 0$  (purely nematic superconductor) we obtain the following inside the superconductor  $|z| > d/2$ :

$$\begin{aligned}H_y &= H(x, y) \left( \sin^2 \alpha_{L(R)} e^{\frac{d/2-|z|}{\lambda_2}} + \cos^2 \alpha_{L(R)} e^{\frac{d/2-|z|}{\lambda_1}} \right), \\ H_x &= \frac{H(x, y) \sin 2\alpha_{L(R)} \left( e^{\frac{d/2-|z|}{\lambda_2}} - e^{\frac{d/2-|z|}{\lambda_1}} \right) \text{sign}(z)}{2}, \\ \lambda_{1,2} &= \frac{c}{4\sqrt{2\pi(J_1 \pm J_4)} e \eta}.\end{aligned}\quad (31)$$

Thus, we obtain an estimate for the London penetration depths  $\lambda_{1,2}$  and observe that the magnetic field in the  $y$  direction in the junction generates the  $x$  component of the field in the bulk. The latter property is a characteristic of anisotropic superconductors [54]. In the considered geometry the anisotropy in the  $(x, y)$  plane arises due to the vector nature of the order parameter.

The relation between the phase difference in the junction and the magnetic field can be derived by different methods giving the same result [1,3,55,56]. We outline briefly one of them.

From the Maxwell equation we have

$$j_x = -\frac{c}{4\pi} \nabla_z H_y, \quad j_y = \frac{c}{4\pi} \nabla_z H_x. \quad (32)$$

We integrate the components of the magnetic field across the junction and using Eqs. (31) obtain

$$\int_{-\infty}^{+\infty} H_y(z) dz = H d_1, \quad \int_{-\infty}^{+\infty} H_x(z) dz = H d_2, \quad (33)$$

where

$$\begin{aligned}d_1 &= d + (\sin^2 \alpha_R + \sin^2 \alpha_L) \lambda_1 + (\cos^2 \alpha_R + \cos^2 \alpha_L) \lambda_2, \\ d_2 &= (\sin 2\alpha_R - \sin 2\alpha_L) (\lambda_2 - \lambda_1) / 2.\end{aligned}\quad (34)$$

The first of these equations is a formal definition of the effective ‘‘magnetic thickness’’ of the junction  $d_1$ . We assume here for definiteness that  $\sin 2\alpha_R - \sin 2\alpha_L > 0$  since the choice of the right and left sides of the junction is arbitrary.

We differentiate Eqs. (32) with respect to  $z$  having in mind that  $\nabla_z \varphi \approx \theta \delta(z)$  if  $\lambda_J \gg \lambda_{1,2}$  [here  $\delta(z)$  is the  $\delta$  function]. Then, we integrate the result with respect to  $z$  from  $z > -z_1$  to  $z < z_1$ , where  $z_1 \gg d_1/2$ . Since  $H_{x,y}(z)$  tends to zero with all its derivatives when  $z \rightarrow \infty$ , we come to the relations

$$\nabla_i \theta = \frac{2\pi}{\Phi_0} \int_{-\infty}^{+\infty} \nabla_z A_i dz, \quad (35)$$

where  $i = x$  and  $y$ . Taking into account that  $H_x = -\nabla_z A_y$  and  $H_y = \nabla_z A_x$ , after integration we derive

$$\nabla_x \theta = \frac{2\pi d_1}{\Phi_0} H(x, y), \quad \nabla_y \theta = \frac{2\pi d_2}{\Phi_0} H(x, y). \quad (36)$$

Finally, using Eqs. (21) and (30) we obtain the equations for  $\theta$  in the following forms:

$$\lambda_J^2 \theta''_{xx} = \sin \theta, \quad (37)$$

$$\theta'_y = \frac{d_2}{d_1} \theta'_x, \quad (38)$$

where we introduce the Josephson length in the usual form [1]

$$\lambda_J = \sqrt{\frac{c\Phi_0}{8\pi^2 d_1 j_{cz} \cos(\alpha_R - \alpha_L)}}. \quad (39)$$

Note that for  $\alpha_R = \alpha_L$  we have  $d_2 = 0$  and  $\theta'_y = 0$ .

Equation (37) is often called the Ferrell-Prange equation [55]. The first of Eqs. (36) relays  $\theta$  and the magnetic field and also gives boundary conditions for  $\theta$  at the edges of the junction where  $H = H_0$ . The values  $\alpha_R$  and  $\alpha_L$  are constants, which depend on the superconducting state in the bulk. We can rewrite the applicability condition of our approach  $\lambda_J \gg \lambda_{1,2}$  in the explicit form using Eqs. (20), (31), and (39):

$$\frac{(J_1 \pm J_4) \sinh \kappa_z d}{J_3 \kappa_z d_1} \gg 1. \quad (40)$$

Now we derive a dependence of the maximum persistent current through the junction  $I_{\max}$  on the applied magnetic field  $H_0$  or on the value of the captured magnetic flux  $\Phi$  [1]. As usual, we consider a short contact in  $x$  and  $y$  directions,  $L_{x,y} \ll 2\lambda_J$ , placed in a sufficiently large magnetic field,  $H_0 \gg \Phi_0/2\pi\lambda_J d_1$ , where  $L_i$  is the junction length in the  $i$ th direction. Within these limits, the magnetic field in the junction is homogeneous and equals the applied field. We integrate the first of Eqs. (36) taking into account that  $H(x, y) = H_0$  and obtain

$$\theta = \frac{2\pi\Phi}{\Phi_0} \left( \frac{x}{L_x} + \frac{d_2 y}{d_1 L_x} \right) + C, \quad (41)$$

where  $\Phi = L_x d_1 H_0$  is the magnetic flux captured in the junction and  $C$  is a constant. We substitute the latter expression in Eq. (21) for the current and integrate it along the junction from  $x = -L_x/2$  to  $x = L_x/2$  and from  $y = -L_y/2$  to  $y = L_y/2$ . We obtain the value of the current through the contact  $I$  in the form

$$\frac{I}{I_{cz}} = \cos(\alpha_L - \alpha_R) \sin C \frac{\sin(\pi\Phi/\Phi_0)}{\pi\Phi/\Phi_0} \frac{\sin(\kappa\pi\Phi/\Phi_0)}{\kappa\pi\Phi/\Phi_0},$$

where  $I_{cz} = j_{cz} d L_x$  and  $\kappa = d_2 L_y / d_1 L_x$ . Thus, the maximum of  $I$  is

$$\frac{I_{\max}}{I_{cz}} = \left| \cos(\alpha_L - \alpha_R) \frac{\sin(\pi\Phi/\Phi_0)}{\pi\Phi/\Phi_0} \frac{\sin(\kappa\pi\Phi/\Phi_0)}{\kappa\pi\Phi/\Phi_0} \right|. \quad (42)$$

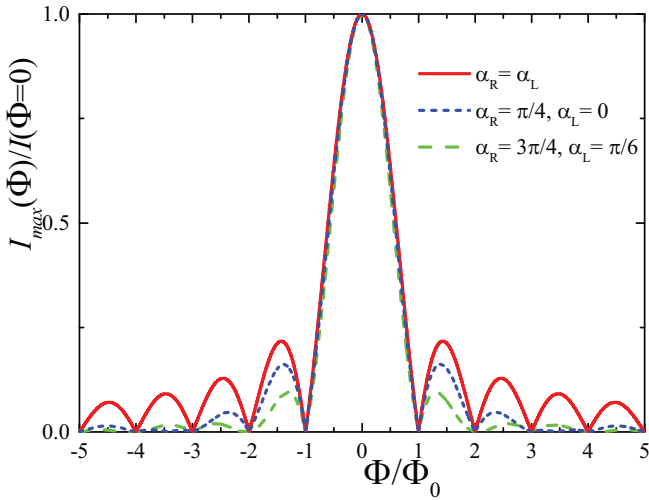


FIG. 5. Dependence of the normalized maximum critical current on the magnetic flux for different nematicity angles  $\alpha_R$  and  $\alpha_L$ . We set  $J_4/J_1 = 3/4$ ,  $L_y = L_x$ , and  $d \ll \lambda_1$ .

The dependence  $I_{\max}(\Phi)$  is shown in Fig. 5. It has a typical Fraunhofer-like pattern, but details of this pattern differ from that for a usual  $s$ -wave superconductor (which corresponds to  $\kappa = 0$  for the considered problem). Mathematically, this difference occurs due to the dependence of the phase  $\theta$  on two coordinates,  $\theta = \theta(x, y)$ . One of the prominent features of the observed picture is that the maximal critical current decays as  $I_{\max} \propto 1/H^2$  instead of  $I_{\max} \propto 1/H$  for the  $s$ -wave superconductors. The period of the current  $I_{\max}(\Phi)$  oscillations depends on the parameters of the system, in particular, on the aspect ratio of the junction  $L_y/L_x$ . The latter feature is illustrated in Fig. 6. The variation of the oscillation period and the  $1/H^2$  decay of the maximum current occurs due to an additional factor  $\sin(\kappa f)/\kappa f$  in Eq. (42), where  $f = \pi \Phi/\Phi_0$ . If  $L_y \ll L_x$ , we get  $\kappa \ll 1$  and  $I_{\max} \propto |\sin f/f|$ , which correspond to the typical Fraunhofer pattern of the

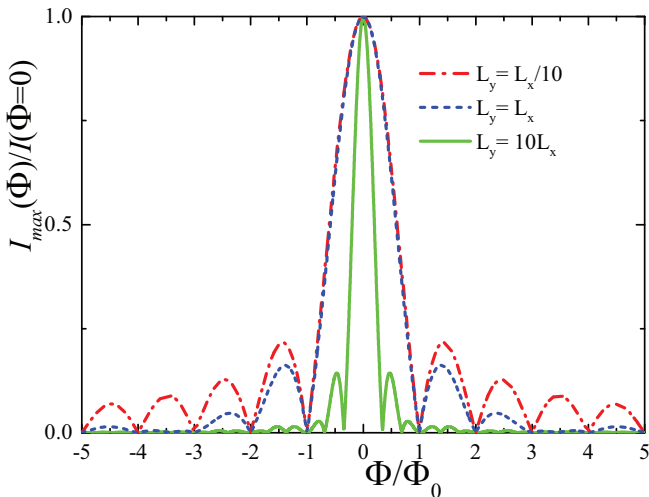


FIG. 6. Dependence of the normalized maximum critical current on the magnetic flux for different values of the aspect ratio of the contact  $L_y/L_x$ . We set  $J_4/J_1 = 3/4$ ,  $\alpha_R = \pi/4$ ,  $\alpha_L = 0$ , and  $d \ll \lambda_1$ .

$s$ -wave superconductor. If  $L_y \gg L_x$  and  $\kappa \gg 1$ , then the period of the oscillations becomes significantly smaller than  $\Phi_0$  when the applied magnetic field is low. Note that we can control the behavior of  $I_{\max}(\Phi)$  rotating the applied field in the junction plane if the values  $L_x$  and  $L_y$  are significantly different.

### B. $x$ junction

Here we consider a junction transverse to the  $x$  axis and the magnetic field lying in the  $(y, z)$  plane,  $\mathbf{H}(x=0) = (0, H_y, H_z)$ , where  $H_y$  and  $H_z$  depend slowly on  $y$  and  $z$ . Using the London equation (16) and following a procedure similar to that for the  $z$  junction, we derive the following for the magnetic field in the bulk of the superconductor:

$$H_y(x) = H_y e^{(d/2-|x|)/\lambda_y}, \quad H_z(x) = H_z e^{(d/2-|x|)/\lambda_z},$$

$$\lambda_y = \frac{c}{4e\eta\sqrt{2\pi J_3}}, \quad (43)$$

$$\lambda_{z,L(R)} = \frac{c}{4e\eta} \sqrt{\frac{J_1 + J_4 \cos 2\alpha_{L(R)}}{2\pi [J_1^2 - J_4^2 (1 - \sin^2 2\alpha_{L(R)} \sin^2 2\delta_{L(R)})]}}$$

where  $\lambda_y$  and  $\lambda_z$  are corresponding London penetration depths ( $\lambda_{y,L} = \lambda_{y,R} = \lambda_y$ ). In the considered case the components of the field decay independently. Similar to the  $z$  junction, we can estimate the effective thickness of the  $x$  junction as  $d_i = d + \lambda_{i,L} + \lambda_{i,R}$  ( $i = y$  and  $z$ ),  $d_y$  corresponds to the applied field along the  $y$  axis and  $d_z$  corresponds to the field along the  $z$  axis.

In the case of the  $x$  junction, the Josephson current has the component along the contact  $j_y(x)$ , Eq. (26). According to Eqs. (15), this current induces a  $z$  component of the magnetic field  $H_z \propto j'_y(x)$ . In general, this field is not negligibly small since  $j'_y(x) \propto j_y/d$ . To avoid this difficulty we consider here only the purely nematic superconductors ( $\delta_{R,L} = 0$ ) and the short junction in a sufficiently large magnetic field, when the magnetic field in the junction is equal to the applied magnetic field. Under these assumptions we can neglect  $j_y$ . Similar to the case of the  $z$  junction we can write the conditions of the applicability of such an approach as [see Eqs. (25) and (39)]  $H_i \gg \Phi_0/2\pi\lambda_{J,i}d_i$  and  $\lambda_i \gg \lambda_{J,i}$ , where

$$\lambda_{J,i} = \sqrt{\frac{c\Phi_0}{8\pi^2 d_i j_{c1} F(\alpha_R, \alpha_L)}},$$

$$F(\alpha_R, \alpha_L) = \cos \alpha_L \cos \alpha_R + \frac{j_{c2}}{j_{c1}} \sin \alpha_L \sin \alpha_R.$$

Now we can derive the dependence of the maximum Josephson current on the magnetic field in the case of the  $x$  junction. We present here the results for two different orientations of the applied magnetic field, along the  $y$  and  $z$  axes. Following the same procedure as in the previous subsection, we readily obtain

$$\nabla_i \theta = \frac{2\pi}{\Phi_0} \int_{-\infty}^{+\infty} \nabla_x A_i dx, \quad (45)$$

where  $i = y$  and  $z$ ,  $H_y = -\nabla_x A_z$ , and  $H_z = \nabla_x A_y$ . After integration over  $x$ , we derive

$$\begin{aligned}\nabla_y \theta &= \frac{2\pi d_y}{\Phi_0} H_z, & \mathbf{H}_0 &= (0, 0, H_z), \\ \nabla_z \theta &= -\frac{2\pi d_z}{\Phi_0} H_y, & \mathbf{H}_0 &= (0, H_y, 0).\end{aligned}\quad (46)$$

These equations relate the phase difference on the junction and the applied magnetic field. Similar to the case of the  $z$  junction, we can derive the dependence of the maximum current on the captured flux in the form

$$\frac{I_{x\max}(\Phi_i)}{I_{c1x}} = F(\alpha_R, \alpha_L) \frac{\sin(\pi \Phi_i / \Phi_0)}{\pi \Phi_i / \Phi_0}, \quad (47)$$

where  $i = y$  and  $z$  and  $I_{c1x} = j_{c1}L$ . Note, that this expression has been obtained under the assumptions of the negligible Josephson Hall current  $j_y$ .

## V. DISCUSSION

One of the key results that we present in this work is that the superconductors with the nematic superconductivity in the  $E_u$  representation have off-diagonal components  $K_{xy}$  in the Meissner kernel [see Eq. (15)]. As a result, we observe the anomalous Josephson Hall effect in the  $x$  junction, that is, the supercurrent flowing along the contact [see Eq. (26) and Fig. 3]. We believe that the nondiagonal Meissner kernel can give rise to other peculiarities in electromagnetic properties of the Josephson junctions. The nature of this Josephson Hall current is different from that of the anomalous Hall effect (AHE), which requires time-reversal symmetry breaking. It is an interesting open question if the presence of the off-diagonal terms in the Meissner kernel that leads to the Josephson Hall effect is related to the topological properties of the normal state and the superconducting order parameter.

In principal, the  $D_{3d}$  symmetry of the topological insulators allows an additional trigonal term in the gradient part of the free energy [36] which is small for the considered materials:

$$\begin{aligned}F_{D,5} &= J_5[(D_z \eta_1)^* D_x \eta_2 + (D_z \eta_2)^* D_x \eta_1 \\ &\times (D_z \eta_1)^* D_y \eta_1 - (D_z \eta_2)^* D_y \eta_2].\end{aligned}\quad (48)$$

As we can see, this term mixes gradients in  $z$  and  $x, y$  directions. In the presence of such a term we have following Meissner kernel:

$$\hat{K} \propto \begin{pmatrix} v_x & \bar{J}_4 & J_5 \sin 2\alpha \cos 2\delta \\ \bar{J}_4 & v_y & J_5 \cos 2\alpha \\ J_5 \sin 2\alpha \cos 2\delta & J_5 \cos 2\alpha & v_z \end{pmatrix}. \quad (49)$$

We see that one component of the vector potential generates three components of the supercurrent if  $J_5 \neq 0$ . It means that not one but two transversal Josephson Hall currents are generated for every orientation of the contact. Values of this new current are proportional to  $J_5$ . If we obtain GL coefficients from the microscopic calculations including only lowest terms in the  $k \cdot p$  expansion, then the  $J_5$  term does not appear [49]. Similar calculations can be performed for the Meissner kernel that yields the same result [51]. So, the absence of the  $J_5$  term results from the high symmetry of the low-energy Hamiltonian of the normal state. This symmetry breaks if we

include hexagonal warping that appears as cubic terms in the expansion. Likely,  $J_5$  emerges due to hexagonal warping terms [57]. On the one hand, it is known that warping is weak in bare  $\text{Bi}_2\text{Se}_3$  [58]. So, it is expected to have  $J_5$  terms to be negligible for low values of the chemical potential. However, in order to achieve the superconductivity, doping shifts the Fermi level away from the charge neutrality point. In this case, the role of the warping increases. It is known that warping significantly affects nematic superconductivity in doped topological insulators [59]. Experimental reconstruction of the Fermi surface of doped topological insulators using ARPES and SdH oscillations does not show any significant warping [60,61]. So, we believe that the  $J_5$  term can be negligible in comparison with the  $J_4$  term for the realistic values of the material parameters.

The current in the junction is controlled by the vector order parameter at each side of the contact  $\vec{\eta} = (\eta_{1R(L)}, \eta_{1L(L)})$ . It is convenient to parametrize the order parameter as  $\vec{\eta} = e^{i\varphi} \eta (\cos \alpha e^{i\delta/2}, \sin \alpha e^{-i\delta/2})$ , where the nematicity direction  $\alpha$  and the phase difference between the order parameter components  $\delta$  determine the vector properties of the order parameter. When  $\delta = 0$ , the nematicity direction  $\alpha$  indicates the direction of the order parameter vector in the coordinate space  $(x, y)$ . The orientation of the order parameter vectors to the contact significantly affects the current in the junction. Thus, we can control the Josephson currents by tuning the nematicity of the superconductors. The simplest strategy to control the nematicity direction is the rotation of the superconductor in the  $(x, y)$  plane. Also, experiments show that large samples of the doped topological insulators are typically multidomain with different orientations of the nematicity vector in each domain. Weak links between different domains are natural objects to study the influence of  $\alpha_{R,L}$  on the Josephson current. The control of the nematicity angle  $\alpha$  by the external strain was demonstrated experimentally (see, e.g., Refs. [26,62]). Thus, we can hope that the variation of the nematicity direction by the applied strain is a feasible task. It opens new possibilities for superconducting devices and also for the detection and study of nematic superconductivity [47,48].

Another parameter that controls the current is the phase difference between order parameters components  $\delta$ . In the case of nonzero  $\delta$  an additional cosine term in the current-phase relations arises [see Eqs. (21) and (25)]. For the pure nematic superconductor, this term vanishes,  $\delta = 0$ . Theoretical analysis shows that the chiral superconducting phase can exist in the systems with an open Fermi surface [44,63], in thin films [64], or under magnetic doping of the nematic superconductor [65,66]. It is argued that in some experiments such a chiral phase with a finite magnetization has been observed [28,30]. However, it is debated in other works [33]. As we show in our previous work, the nonzero  $\delta$  can be caused in the nematic phase by the external magnetization [43]. The value of  $\delta$  induced by the magnetization is small [44]. However, measurements of the currents in the Josephson junctions can be performed with high accuracy. We believe that the observation of the cosine term in the current that is caused by the magnetization is experimentally possible.

We observe that in the  $x$  junction the Josephson Hall current along the junction,  $j_y$ , can be generated as well as

the current across the junction,  $j_x$ . In some cases  $j_y$  can be larger than  $j_x$ . Consider a junction made of two pure nematic superconductors with the order parameters  $\vec{\eta}_L = \eta(1, 0)$  and  $\vec{\eta}_R = \eta e^{i\theta}(0, 1)$  that are orthogonal to each other and one of them is parallel to the contact plane. In this case, the longitudinal current vanishes,  $j_x = 0$  [see Eq. (25)], but transverse current is nonzero,  $j_y = j_{cy} \sin \theta$  [see Eq. (28)].

An analysis of Eq. (26) shows that under definite conditions the Josephson Hall current does not necessary decay exponentially with the increase of the junction thickness  $d$  if  $\delta_L$  and/or  $\delta_R$  is nonzero. In the leading approximation with respect to  $\kappa_i d \gg 1$ , we obtain that  $d \bar{j}_y \propto J_4 \text{Im}(\eta_{1L}^* \eta_{2L} - \eta_{1R}^* \eta_{2R})$ , which is nonzero for  $d \rightarrow +\infty$ . For example, such a situation takes place when  $\delta \neq 0$  only on one side of the junction, which can be due to its magnetization or when one side of the junction is the chiral superconductor  $\vec{\eta}_L \propto (1, i)$  and another side is nematic. It is worth mentioning that the Hall current flows even if we consider a single boundary of the chiral superconductor, e.g.,  $\vec{\eta}_R = (0, 0)$ . Moreover, if  $\delta$  in the superconductor is nonzero, then a finite current flows along the edge,  $d \bar{j}_y \propto J_4 \eta_L^2 \sin 2\alpha_L \sin \delta_L$ . Note that a similar type of superconducting anomalous Hall effect has been predicted for a chiral  $p$ -wave superconductor [67].

In Refs. [6–14] the anomalous Josephson Hall effect has been considered in the materials with a finite magnetization. This magnetization brings asymmetry to the Andreev bound states spectra that results in a finite Josephson Hall current. In our case, this supercurrent exists without magnetization. Thus, we establish that the anomalous Josephson Hall effect can be realized without any magnetization while time-reversal symmetry breaking occurs due to the phase difference across the contact.

One of the distinct features of London equations is the lack of gauge invariance for the current that leads to the lack of the charge conservation [68,69]. Usually, it is not a problem when the Meissner kernel is diagonal since we can always choose the proper gauge for a vector potential where the charge is locally conserved. In our case, we get formally that the charge is not conserved in the case of the  $x$  junction if  $\theta = \theta(y)$ , which is the case for the  $z$  direction of the magnetic field. This drawback cannot be cured in a GL formalism. Instead, we

should perform microscopic calculations of the current that include vertex corrections for a current operator that arises due to mean-field self-energy and Coulomb interaction. After that a global gauge invariance is restored and reliable results are obtained for any gauge of the vector potential [68,69]. In the case of the anomalous superconducting Hall effect, restoring the gauge invariance leads to the large additional quasiparticle contribution to the edge current [70]. It means that the anomalous Hall supercurrent is significantly renormalized by the vertex corrections. Thus, we expect a strong renormalization by the vertex corrections of the Josephson Hall current  $j_y$  in the  $x$  contact as well. However, microscopic calculations that include vertex corrections are beyond the scope of this paper.

The results of our work can be easily generalized to other nontrivial superconductors that have a nondiagonal Meissner kernel. Such a nondiagonal kernel arises due to finite mixing terms  $(D_i \eta_\alpha)^* D_j \eta_\beta$  in the GL functional. In the case considered here, the mixing terms are proportional the GL coefficient  $J_4$ . The GL functional with such mixing terms has been proposed for  $p$ -wave superconductivity in  $\text{Sr}_2\text{RuO}_4$  [71] and in uranium superconductors [72] and is typical for the superconductors with the triplet pairing [73].

In conclusion, we study electromagnetic properties of the Josephson junction between two nematic superconductors in the Ginzburg-Landau approach. We derive the London equations for the nematic superconductor with odd  $E_u$  pairing using the second GL equation. We observe that the Meissner kernel has off-diagonal components. Using this result, we obtain current-phase relations for different orientations of the junction plane, crystallographic axes of the sample, and the nematicity vector. We show that the anomalous Josephson Hall effect can be observed in the absence of magnetization. We calculate the magnetic field dependence of the maximum current through the junction. We show that the period of the Fraunhofer oscillations depends on the geometry of the junction, the direction of the magnetic field, and the nematicity vector.

## ACKNOWLEDGMENTS

R.S.A. acknowledges the support by the Russian Science Foundation (Project No. 22-72-00032).

- 
- [1] A. Barone and G. Paterno, *Physics and Applications of the Josephson Effect* (Wiley Online Library, Hoboken, NJ, 1982), Vol. 1.
  - [2] M. Tinkham, *Introduction to Superconductivity*, 2nd ed. (Dover, New York, 2004).
  - [3] K. K. Likharev, Superconducting weak links, *Rev. Mod. Phys.* **51**, 101 (1979).
  - [4] F. Tafuri, *Fundamentals and Frontiers of the Josephson Effect*, Springer Series in Materials Science Vol. 286 (Springer Nature, Cham, Switzerland, 2019).
  - [5] B. Baek, W. H. Rippard, S. P. Benz, S. E. Russek, and P. D. Dresselhaus, Hybrid superconducting-magnetic memory device using competing order parameters, *Nat. Commun.* **5**, 3888 (2014).
  - [6] J. Wang, L. Hao, Y. H. Yang, and K. S. Chan, Josephson hall current in a noncentrosymmetric superconductor/ferromagnet/superconductor junction, *J. Appl. Phys.* **110**, 113717 (2011).
  - [7] A. Vedyayev, N. Ryzhanova, N. Strelkov, and B. Dieny, Spontaneous Anomalous and Spin Hall Effects Due to Spin-Orbit Scattering of Evanescent Wave Functions in Magnetic Tunnel Junctions, *Phys. Rev. Lett.* **110**, 247204 (2013).
  - [8] T. Yokoyama, Anomalous Josephson Hall effect in magnet/triplet superconductor junctions, *Phys. Rev. B* **92**, 174513 (2015).
  - [9] A. Matos-Abiague and J. Fabian, Tunneling Anomalous and Spin Hall Effects, *Phys. Rev. Lett.* **115**, 056602 (2015).

- [10] T. H. Dang, H. Jaffrès, T. L. Hoai Nguyen, and H.-J. Drouhin, Giant forward-scattering asymmetry and anomalous tunnel Hall effect at spin-orbit-split and exchange-split interfaces, *Phys. Rev. B* **92**, 060403(R) (2015).
- [11] S. Mironov and A. Buzdin, Spontaneous Currents in Superconducting Systems with Strong Spin-Orbit Coupling, *Phys. Rev. Lett.* **118**, 077001 (2017).
- [12] A. G. Mal'shukov, AC anomalous hall effect in topological insulator Josephson junctions, *Phys. Rev. B* **100**, 035301 (2019).
- [13] A. Costa and J. Fabian, Anomalous Josephson Hall effect charge and transverse spin currents in superconductor/ferromagnetic-insulator/superconductor junctions, *Phys. Rev. B* **101**, 104508 (2020).
- [14] O. Maistrenko, B. Scharf, D. Manske, and E. M. Hankiewicz, Planar Josephson Hall effect in topological Josephson junctions, *Phys. Rev. B* **103**, 054508 (2021).
- [15] N. Nagaosa, J. Sinova, S. Onoda, A. H. MacDonald, and N. P. Ong, Anomalous Hall effect, *Rev. Mod. Phys.* **82**, 1539 (2010).
- [16] Y. S. Hor, A. J. Williams, J. G. Checkelsky, P. Roushan, J. Seo, Q. Xu, H. W. Zandbergen, A. Yazdani, N. P. Ong, and R. J. Cava, Superconductivity in  $\text{Cu}_x\text{Bi}_2\text{Se}_3$  and Its Implications for Pairing in the Undoped Topological Insulator, *Phys. Rev. Lett.* **104**, 057001 (2010).
- [17] S. Sasaki, M. Kriener, K. Segawa, K. Yada, Y. Tanaka, M. Sato, and Y. Ando, Topological Superconductivity in  $\text{Cu}_x\text{Bi}_2\text{Se}_3$ , *Phys. Rev. Lett.* **107**, 217001 (2011).
- [18] T. Kirzchner, E. Lahoud, K. B. Chaska, Z. Salman, and A. Kanigel, Point-contact spectroscopy of  $\text{Cu}_{0.2}\text{Bi}_2\text{Se}_3$  single crystals, *Phys. Rev. B* **86**, 064517 (2012).
- [19] T. Kawai, C. G. Wang, Y. Kandori, Y. Honoki, K. Matano, T. Kambe, and G. qing Zheng, Direction and symmetry transition of the vector order parameter in topological superconductors  $\text{Cu}_x\text{Bi}_2\text{Se}_3$ , *Nat. Commun.* **11**, 235 (2020).
- [20] S. Yonezawa, K. Tajiri, S. Nakata, Y. Nagai, Z. Wang, K. Segawa, Y. Ando, and Y. Maeno, Thermodynamic evidence for nematic superconductivity in  $\text{Cu}_x\text{Bi}_2\text{Se}_3$ , *Nat. Phys.* **13**, 123 (2017).
- [21] R. Tao, Y.-J. Yan, X. Liu, Z.-W. Wang, Y. Ando, Q.-H. Wang, T. Zhang, and D.-L. Feng, Direct Visualization of the Nematic Superconductivity in  $\text{Cu}_x\text{Bi}_2\text{Se}_3$ , *Phys. Rev. X* **8**, 041024 (2018).
- [22] K. Matano, M. Kriener, K. Segawa, Y. Ando, and G. qing Zheng, Spin-rotation symmetry breaking in the superconducting state of  $\text{Cu}_x\text{Bi}_2\text{Se}_3$ , *Nat. Phys.* **12**, 852 (2016).
- [23] Shruti, V. K. Maurya, P. Neha, P. Srivastava, and S. Patnaik, Superconductivity by Sr intercalation in the layered topological insulator  $\text{Bi}_2\text{Se}_3$ , *Phys. Rev. B* **92**, 020506(R) (2015).
- [24] Z. Liu, X. Yao, J. Shao, M. Zuo, L. Pi, S. Tan, C. Zhang, and Y. Zhang, Superconductivity with topological surface state in  $\text{Sr}_x\text{Bi}_2\text{Se}_3$ , *J. Am. Chem. Soc.* **137**, 10512 (2015).
- [25] A. Y. Kuntsevich, M. A. Bryzgalov, V. A. Prudkoglyad, V. P. Martovitskii, Y. G. Selivanov, and E. G. Chizhevskii, Structural distortion behind the nematic superconductivity in  $\text{Sr}_x\text{Bi}_2\text{Se}_3$ , *New J. Phys.* **20**, 103022 (2018).
- [26] A. Y. Kuntsevich, M. A. Bryzgalov, R. S. Akzyanov, V. P. Martovitskii, A. L. Rakhmanov, and Y. G. Selivanov, Strain-driven nematicity of odd-parity superconductivity in  $\text{Sr}_x\text{Bi}_2\text{Se}_3$ , *Phys. Rev. B* **100**, 224509 (2019).
- [27] Y. Pan, A. M. Nikitin, G. K. Araizi, Y. K. Huang, Y. Matsushita, T. Naka, and A. de Visser, Rotational symmetry breaking in the topological superconductor  $\text{Sr}_x\text{Bi}_2\text{Se}_3$  probed by upper-critical field experiments, *Sci. Rep.* **6**, 28632 (2016).
- [28] P. Neha, P. K. Biswas, T. Das, and S. Patnaik, Time-reversal symmetry breaking in topological superconductor  $\text{Sr}_{0.1}\text{Bi}_2\text{Se}_3$ , *Phys. Rev. Mater.* **3**, 074201 (2019).
- [29] M. I. Bannikov, R. S. Akzyanov, N. K. Zhurbina, S. I. Khaldeev, Y. G. Selivanov, V. V. Zavalov, A. L. Rakhmanov, and A. Y. Kuntsevich, Breaking of Ginzburg-Landau description in the temperature dependence of the anisotropy in a nematic superconductor, *Phys. Rev. B* **104**, L220502 (2021).
- [30] Y. Qiu, K. N. Sanders, J. Dai, J. E. Medvedeva, W. Wu, P. Ghaemi, T. Vojta, and Y. S. Hor, Time reversal symmetry breaking superconductivity in topological materials, [arXiv:1512.03519](https://arxiv.org/abs/1512.03519).
- [31] C. Kurter, A. D. K. Finck, E. D. Huemiller, J. Medvedeva, A. Weis, J. M. Atkinson, Y. Qiu, L. Shen, S. H. Lee, T. Vojta, P. Ghaemi, Y. S. Hor, and D. J. V. Harlingen, Conductance spectroscopy of exfoliated thin flakes of  $\text{Nb}_x\text{Bi}_2\text{Se}_3$ , *Nano Lett.* **19**, 38 (2019).
- [32] T. Asaba, B. J. Lawson, C. Tinsman, L. Chen, P. Corbae, G. Li, Y. Qiu, Y. S. Hor, L. Fu, and L. Li, Rotational Symmetry Breaking in a Trigonal Superconductor Nb-Doped  $\text{Bi}_2\text{Se}_3$ , *Phys. Rev. X* **7**, 011009 (2017).
- [33] D. Das, K. Kobayashi, M. P. Smylie, C. Mielke, T. Takahashi, K. Willa, J.-X. Yin, U. Welp, M. Z. Hasan, A. Amato, H. Luetkens, and Z. Guguchia, Time-reversal invariant and fully gapped unconventional superconducting state in the bulk of the topological compound  $\text{Nb}_{0.25}\text{Bi}_2\text{Se}_3$ , *Phys. Rev. B* **102**, 134514 (2020).
- [34] L. Fu and E. Berg, Odd-Parity Topological Superconductors: Theory and Application to  $\text{Cu}_x\text{Bi}_2\text{Se}_3$ , *Phys. Rev. Lett.* **105**, 097001 (2010).
- [35] L. Fu, Odd-parity topological superconductor with nematic order: Application to  $\text{Cu}_x\text{Bi}_2\text{Se}_3$ , *Phys. Rev. B* **90**, 100509(R) (2014).
- [36] J. W. F. Venderbos, V. Kozii, and L. Fu, Identification of nematic superconductivity from the upper critical field, *Phys. Rev. B* **94**, 094522 (2016).
- [37] S. Yonezawa, Nematic superconductivity in doped  $\text{Bi}_2\text{Se}_3$  topological superconductors, *Condensed Matter* **4**, 2 (2018).
- [38] F. Wu and I. Martin, Majorana Kramers pair in a nematic vortex, *Phys. Rev. B* **95**, 224503 (2017).
- [39] R. S. Akzyanov and A. L. Rakhmanov, Strain-induced spin vortex and majorana Kramers pairs in doped topological insulators with nematic superconductivity, *Phys. Rev. B* **104**, 094511 (2021).
- [40] M. Hecker and J. Schmalian, Vestigial nematic order and superconductivity in the doped topological insulator  $\text{Cu}_x\text{Bi}_2\text{Se}_3$ , *npj Quantum Mater.* **3**, 26 (2018).
- [41] L. Hao and C. S. Ting, Nematic superconductivity in  $\text{Cu}_x\text{Bi}_2\text{Se}_3$ : Surface Andreev bound states, *Phys. Rev. B* **96**, 144512 (2017).
- [42] H. Uematsu, T. Mizushima, A. Tsuruta, S. Fujimoto, and J. A. Sauls, Chiral Higgs Mode in Nematic Superconductors, *Phys. Rev. Lett.* **123**, 237001 (2019).
- [43] R. S. Akzyanov, A. V. Kapranov, and A. L. Rakhmanov, Spontaneous strain and magnetization in doped topological

- insulators with nematic and chiral superconductivity, *Phys. Rev. B* **102**, 100505(R) (2020).
- [44] D. A. Khokhlov and R. S. Akzyanov, Pauli paramagnetism of triplet Cooper pairs in a nematic superconductor, *Phys. Rev. B* **104**, 214514 (2021).
- [45] M. Chen, X. Chen, H. Yang, Z. Du, and H.-H. Wen, Superconductivity with twofold symmetry in  $\text{Bi}_2\text{Te}_3/\text{FeTe}_{0.55}\text{Se}_{0.45}$  heterostructures, *Sci. Adv.* **4**, eaat1084 (2018).
- [46] D. A. Khokhlov and R. S. Akzyanov, Quasiparticle interference in doped topological insulators with nematic superconductivity, *Phys. E* **133**, 114800 (2021).
- [47] P. T. How and S.-K. Yip, Signatures of nematic superconductivity in doped  $\text{Bi}_2\text{Se}_3$  under applied stress, *Phys. Rev. B* **100**, 134508 (2019).
- [48] H.-B. Leng, C. Li, and X. Liu, Reveal the nematic topological superconductivity from the anisotropic unconventional Josephson effect: Theory and application to doped  $\text{Bi}_2\text{Se}_3$ , *Sci. China Phys. Mech. Astron.* **64**, 297211 (2021).
- [49] A. A. Zyuzin, J. Garaud, and E. Babaev, Nematic Skyrmions in Odd-Parity Superconductors, *Phys. Rev. Lett.* **119**, 167001 (2017).
- [50] J. Schmidt, F. Parhizgar, and A. M. Black-Schaffer, Odd-frequency superconductivity and Meissner effect in the doped topological insulator  $\text{Bi}_2\text{Se}_3$ , *Phys. Rev. B* **101**, 180512(R) (2020).
- [51] R. S. Akzyanov, Lifshitz transition in dirty doped topological insulator with nematic superconductivity, *Phys. Rev. B* **104**, 224502 (2021).
- [52] A. Buzdin, Direct Coupling between Magnetism and Superconducting Current in the Josephson  $\varphi_0$  Junction, *Phys. Rev. Lett.* **101**, 107005 (2008).
- [53] A. Sasaki, S. Ikegaya, T. Habe, A. A. Golubov, and Y. Asano, Josephson effect in two-band superconductors, *Phys. Rev. B* **101**, 184501 (2020).
- [54] V. G. Kogan, London approach to anisotropic type-II superconductors, *Phys. Rev. B* **24**, 1572 (1981).
- [55] R. A. Ferrell and R. E. Prange, Self-Field Limiting of Josephson Tunneling of Superconducting Electron Pairs, *Phys. Rev. Lett.* **10**, 479 (1963).
- [56] I. O. Kulik and I. K. Yanson, *Josephson Effect in Superconducting Tunneling Structures* (Wiley & Sons, New York, 1972).
- [57] C.-X. Liu, X.-L. Qi, H. J. Zhang, X. Dai, Z. Fang, and S.-C. Zhang, Model Hamiltonian for topological insulators, *Phys. Rev. B* **82**, 045122 (2010).
- [58] K. Kuroda, M. Arita, K. Miyamoto, M. Ye, J. Jiang, A. Kimura, E. E. Krasovskii, E. V. Chulkov, H. Iwasawa, T. Okuda, K. Shimada, Y. Ueda, H. Namatame, and M. Taniguchi, Hexagonally Deformed Fermi Surface of the 3D Topological Insulator  $\text{Bi}_2\text{Se}_3$ , *Phys. Rev. Lett.* **105**, 076802 (2010).
- [59] R. S. Akzyanov, D. A. Khokhlov, and A. L. Rakhmanov, Nematic superconductivity in topological insulators induced by hexagonal warping, *Phys. Rev. B* **102**, 094511 (2020).
- [60] E. Lahoud, E. Maniv, M. S. Petrushevsky, M. Naamneh, A. Ribak, S. Wiedmann, L. Petaccia, Z. Salman, K. B. Chashka, Y. Dagan, and A. Kanigel, Evolution of the Fermi surface of a doped topological insulator with carrier concentration, *Phys. Rev. B* **88**, 195107 (2013).
- [61] A. Almoalem, I. Silber, S. Sandik, M. Lotem, A. Ribak, Y. Nitzav, A. Y. Kuntsevich, O. A. Sobolevskiy, Y. G. Selivanov, V. A. Prudkoglyad, M. Shi, L. Petaccia, M. Goldstein, Y. Dagan, and A. Kanigel, Link between superconductivity and a Lifshitz transition in intercalated  $\text{Bi}_2\text{Se}_3$ , *Phys. Rev. B* **103**, 174518 (2021).
- [62] I. Kostylev, S. Yonezawa, Z. Wang, Y. Ando, and Y. Maeno, Uniaxial-strain control of nematic superconductivity in  $\text{Sr}_x\text{Bi}_2\text{Se}_3$ , *Nat. Commun.* **11**, 4152 (2020).
- [63] J. W. F. Venderbos, V. Kozii, and L. Fu, Odd-parity superconductors with two-component order parameters: Nematic and chiral, full gap, and majorana node, *Phys. Rev. B* **94**, 180504(R) (2016).
- [64] L. Chirolli, Chiral superconductivity in thin films of doped  $\text{Bi}_2\text{Se}_3$ , *Phys. Rev. B* **98**, 014505 (2018).
- [65] L. Chirolli, F. de Juan, and F. Guinea, Time-reversal and rotation symmetry breaking superconductivity in Dirac materials, *Phys. Rev. B* **95**, 201110(R) (2017).
- [66] N. F. Q. Yuan, W.-Y. He, and K. T. Law, Superconductivity-induced ferromagnetism and Weyl superconductivity in Nb-doped  $\text{Bi}_2\text{Se}_3$ , *Phys. Rev. B* **95**, 201109(R) (2017).
- [67] A. Furusaki, M. Matsumoto, and M. Sigrist, Spontaneous Hall effect in a chiral  $p$ -wave superconductor, *Phys. Rev. B* **64**, 054514 (2001).
- [68] Y. Nambu, Quasi-particles and gauge invariance in the theory of superconductivity, *Phys. Rev.* **117**, 648 (1960).
- [69] J. R. Schrieffer, *Theory of Superconductivity* (Benjamin, San Francisco, 1964).
- [70] M. Stone and R. Roy, Edge modes, edge currents, and gauge invariance in  $p_x + ip_y$  superfluids and superconductors, *Phys. Rev. B* **69**, 184511 (2004).
- [71] R. Heeb and D. F. Agterberg, Ginzburg-Landau theory for a  $p$ -wave  $\text{Sr}_2\text{RuO}_4$  superconductor: Vortex core structure and extended London theory, *Phys. Rev. B* **59**, 7076 (1999).
- [72] D. F. Agterberg and M. J. W. Dodgson, London Theory for Superconducting Phase Transitions in External Magnetic Fields: Application to  $\text{UPt}_3$ , *Phys. Rev. Lett.* **89**, 017004 (2002).
- [73] F. N. Krogh and A. Sudbø, Derivation of a Ginzburg-Landau free energy density of a  $p + ip$  superconductor from spin-orbit coupling with mixed gradient terms, *Phys. Rev. B* **98**, 014510 (2018).